JOURNAL OF THERMOPHYSICS AND HEAT TRANSFER
Vol. 7, No. 1, Jan.–March 1993

# Numerical Study of Mixed Convection Between Two Corotating Symmetrically Heated Disks

C. Y. Soong*
*Chung Cheng Institute of Technology, Taoyuan, Taiwan 33509, Republic of China*
and
W. M. Yan†
*Hua Fan Institute of Technology, Taipei, Taiwan 22305, Republic of China*

**This article is concerned with a numerical study of mixed convection between two symmetrically heated corotating disks. Both thermal boundary conditions of constant wall temperature and uniform heat flux are considered. By applying the boundary-layer approximation and a linear relation for density variation in centrifugal force term, the governing equations reduce to a Boussinesq system of parabolic nature. The spatially developing flow and heat transfer are studied numerically. The effects of centrifugal buoyancy, Coriolis force, radial through-flow, and wall-heating on the flow structure and heat transfer performance are examined in detail. The results reveal that the centrifugal buoyancy, which was ignored in prior studies, is indeed a significant effect in this class of rotating flows.**

## Nomenclature

$C_f$ = skin friction coefficient, $\mu(\partial u/\partial z)_w/(\rho u_{in}^2/2)$
$Gr_\Omega$ = rotational Grashof number, $(\Omega^2 s)\beta\Delta T_c s^3/\nu^2$
$h$ = heat transfer coefficient, W/(m²K)
$k$ = thermal conductivity, W/(mK)
$Nu$ = Nusselt number, $hs/k$
$P$ = static pressure, N/m²
$Pe$ = Peclect number, $PrRe$
$Pr$ = Prandtl number, $\nu/\alpha$
$P'$, $p'$ = dimensionless and dimensional pressure departure, respectively, $P' = p'/\rho u_{in}^2$
$q''$ = heat flux, W/(m²s)
$R$, $r$ = dimensionless and dimensional radial coordinate, respectively, $R = r/s$
$Re$ = through-flow Reynolds number based on inlet velocity, $u_{in}s/\nu$
$Re_\varphi$ = tip Reynolds number, $r_0^2\Omega/\nu = ReRoR_0^2$
$Re_\Omega$ = rotational Reynolds number, $\Omega_s^2/\nu = ReRo$
$Ro$ = rotation number, $\Omega s/u_{in}$
$R'$ = dimensionless relative radial position, $(r - r_{in})/s$
$s$ = disk spacing, m
$T$ = temperature, K
$U$, $V$, $W$ = dimensionless velocity components, $u/u_{in}$, $v/u_{in}$, $w/u_{in}$
$u$, $v$, $w$ = dimensional velocity components, m/s
$Z$, $z$ = dimensionless and dimensional axial coordinate, $Z = z/s$
$\alpha$ = thermal diffusivity, m²/s
$\beta$ = thermal expansion coefficient, 1/K
$\Delta T_c$ = characteristic temperature difference, $(T_w - T_{in})$ for UWT and $(q_w''s/k)$ for UHF, °C or K
$\theta$ = dimensionless temperature difference, $(T - T_{in})/\Delta T_c$
$\mu$ = viscosity, Ns/m²
$\nu$ = kinematic viscosity, m²/s
$\rho$ = density, kg/m³
$\Omega$ = rotational speed, 1/s or rpm

*Subscripts*
in = inlet
$o$ = outer
$r$ = reference
$w$ = wall

*Superscript*
$\bar{}$ = mean

## Introduction

FLUID flow and heat transfer in rotating disk systems has attracted much attention due to its relevance to many engineering problems. Numerous investigations were conducted for various thermal systems, e.g., gas turbine and compressor disks,[1-4] rotating fin heat exchangers,[5] rotating disk contactors,[6] and magnetic disk storage systems.[7] Recently, in their monograph, Owen and Rogers[8] reviewed the previous studies on flow and heat transfer (pure forced convection) in rotating disk systems. Cold air can be introduced between the corotating disks in rotating devices and used for disk cooling. To a rotating frame of reference two extra forces, Coriolis and centrifugal, appear in the momentum balance of the fluid flow. Under the condition of rotational speed of $10^3$ rpm, e.g., the order of the centrifugal acceleration is about $10^2$ $g$ (gravity) at a radial position of 0.1 m. The buoyancy effect due to this large body force may become significant and could be expected to alter the flow and temperature fields. In radially rotating channels, the centrifugal-buoyancy effect on heat transfer has been extensively studied, both analytically[9-11] and experimentally.[12,13] However, for rotating disk systems, this rotation-induced buoyancy effect has usually been ignored in previous studies (either theoretical/numerical or experimental).

In the present study, emphasis is placed on the numerical study of rotational effects, especially the centrifugal-buoyancy effect, on the fluid flow and heat transfer characteristics in rotating disk systems. The buoyancy effect can be taken into account by invoking Boussinesq's approximation to the centrifugal force term in the momentum equation. In his study Raal[14] found that even at Reynolds numbers as low as $Re \sim O(10^2)$, the classical boundary-layer theory can give a valid approximation in the nonseparated flow region between parallel disks. To save the computer memory and reduce the

Received Aug. 23, 1991; revision received Jan. 27, 1992; accepted for publication Feb. 4, 1992. 

*Associate Professor, Department of Aeronautical Engineering. Member AIAA.
†Associate Professor, Department of Mechanical Engineering.

computational effort, the boundary-layer approximation is employed in the present work. The resultant parabolic system is solved by using a marching technique. The symmetric flow configuration considered in Sim and Yang's study[15] is adopted. To demonstrate the validity of the present calculation procedure, the solutions are compared with the elliptic ones in Ref. 15. The Reynolds numbers and rotation numbers are restricted to the ranges of $Re \leq 1000$ and $Ro \sim O(10^{-2})$ to avoid transition and turbulence, which are beyond the scope of this investigation. The effects of centrifugal buoyancy, Coriolis force, and through-flow on the flow and heat transfer characteristics are presented. Two symmetric wall-heating conditions 1) uniform wall temperature (UWT); and 2) uniform heat flux (UHF), are considered to examine the influence of rotation under various thermal conditions.

## Analysis

### Problem Statement

The flow configuration considered in the present study is schematically shown in Fig. 1. Two coaxial disks with an outer diameter of $2r_0$ and an opening $2r_{in}$ at the center are separated by a spacing $s$. The disk system rotates at a constant speed $\Omega$. Coolant fluid at uniform inlet velocity $u_{in}$ flows radially outwards through the space between the disks. The inlet fluid is of uniform temperature $T_{in}$ and both of the disks are symmetrically heated to a constant temperature $T_w$ (isothermal disks) or at a uniform heat flux $q''_w$ (isoflux disks). As shown in Fig. 1, a cylindrical coordinate system $(r, z)$ is fixed on one of the disks, e.g., disk 1, with origin at the disk center. The fluid flow under consideration is assumed to be steady, laminar, axisymmetric, and of constant physical properties. The boundary-layer approximation is used as a simplification in this coupled flow and heat transfer problem. To consider the buoyancy effect, Boussinesq's approximation is invoked and the linear relation $\rho = \rho_r[1 - \beta(T - T_r)]$, is used to allow for the density variation in the centrifugal force terms. In this case gravitational effects are comparatively small and can be neglected.

Under the above conditions and assumptions the dimensionless governing equations can be written as

$$\frac{\partial(RU)}{\partial R} + \frac{\partial(RW)}{\partial Z} = 0 \tag{1}$$

$$U\frac{\partial U}{\partial R} - \frac{V^2}{R} + W\frac{\partial U}{\partial Z} = \frac{1}{Re}\frac{\partial^2 U}{\partial Z^2} + 2RoV - \frac{Gr_\Omega}{Re^2}R\theta - \frac{\partial P'}{\partial R} \tag{2}$$

$$U\frac{\partial V}{\partial R} + W\frac{\partial V}{\partial Z} + \frac{UV}{R} = \frac{1}{Re}\frac{\partial^2 V}{\partial Z^2} - 2RoU \tag{3}$$

$$U\frac{\partial \theta}{\partial R} + W\frac{\partial \theta}{\partial Z} = \frac{1}{Pe}\frac{\partial^2 \theta}{\partial Z^2} \tag{4}$$

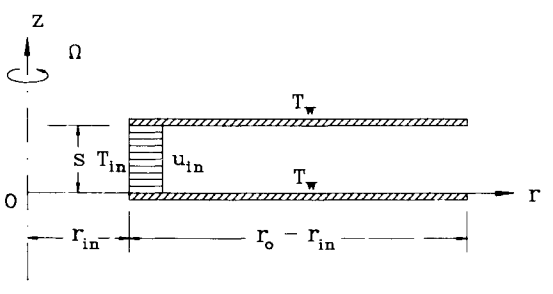


**Fig. 1 Schematic diagram of the flow configuration.**

The overall mass balance is

$$\int_0^{1/2} RU\, dZ = R_{in} \tag{5}$$

Because the problem is parabolic in the radial direction, inlet conditions are needed to start the marching procedure. The upper bound of the solution domain is the centerline where the symmetric conditions are imposed. The lower bound is the disk containing the rotating reference frame. The dimensionless boundary conditions, therefore, can be expressed as

$$R = R_{in}: \quad U - 1 = V = W = \theta = 0$$

$$Z = \tfrac{1}{2}: \quad \partial U/\partial Z = \partial V/\partial Z = W = \partial\theta/\partial Z = 0 \tag{6}$$

$$Z = 0: \quad U = V = W = 0; \quad \text{and} \quad \begin{cases} \theta = 1 & \text{(UWT)} \\ \dfrac{\partial\theta}{\partial Z} = 1 & \text{(UHF)} \end{cases}$$

### Governing Parameters

The governing parameters in this problem are the inner and outer radii $R_{in}$ and $R_0$, respectively, the Pradtl number $Pr$, the through-flow Reynolds number $Re$, the rotation number $Ro$, and the rotational Grashof number $Gr_\Omega$. The radii $R_{in}$ and $R_0$ are geometric parameters. Considering air as the working fluid, $Pr$ of 0.7 was used in the computations. $Re$ represents the forced flow effect, and the last two $Ro$ and $Gr_\Omega$ characterize the effects of Coriolis force and centrifugal buoyancy, respectively. Note that the terms $2RoV$ and $-2RoU$, the dimensionless components of the vector $-2\boldsymbol{\Omega} \times \boldsymbol{V}$, in the momentum equations are usually referred to as the Coriolis terms.[8] Although in some literature[16] the radial component $2RoV$ is claimed as a force of Coriolis structure but of centrifugal nature, the conventional terminology "Coriolis term" will be used herein to distinguish its effects from that of the centrifugal force $R\Omega^2$. It is observed that from the buoyancy term $(Gr_\Omega/Re^2)R\theta$ in Eq. (2), both the parameter group $(Gr_\Omega/Re^2)$ and the length scale in radial direction (e.g., $R_0$) are related to the buoyancy effects. The magnitude of the rotational Grashof number depends on the rotational speed and temperature difference. The orientation of the main flow, radially inward or outward, and the thermal condition, heated wall or cooled wall, determine the sign of $Gr_\Omega$. The positive $Gr_\Omega$ corresponds to the buoyancy effect retarding the main flow, and the negative one corresponds to that assisting the main flow.

The order of magnitude of the governing parameters is now checked. Consider a rotating fin heat exchanger with fin spacing $s = 3 \times 10^{-3}$ m, $\Delta T_c = 60°C$, and rotating angular speed $\Omega = 1000$ rpm. For stable laminar flows, the limiting flow and rotational conditions are $Re < 1200$[17,18] and $Re_\Omega < 20$ for corotating disks of outer radius $R_0 = 118.5$.[18] For smaller disks the rotational condition may be released for lower tip velocity. An alternative rotational parameter, the tip Reynolds number $Re_\varphi \equiv r_0^2\Omega/\nu = Re_\Omega R_0^2$, which is a combination of the rotational and the geometric parameters, may be more useful. The critical condition for stable laminar flow in rotating disk systems is $Re_\varphi \sim O(10^5)$[8]. Similarly, the recent experimental work[18] provided a critical condition of the same order $Re_\varphi = 2.8 \times 10^5$. Accordingly, the Reynolds number $Re \leq 1000$ and the rotation numbers of $O(10^{-2})$, e.g., $0 \leq Ro \leq 0.08$, are appropriate in laminar flow calculations. For example, in a case of $Re = 1000$, $Ro = 0.05$, and $R_0 = 60$, $Re_\varphi$ is $1.8 \times 10^5$ and lies in laminar flow regime. Evaluating physical properties at the reference condition $T_r = 293$ K, the rotational Grashof number is $Gr_\Omega \approx 800$. In this study the range of rotational Grashof numbers is $-1500 \leq Gr_\Omega \leq 1500$. For high-buoyancy cases in the present calculations, $Re$

= 250, $Gr_\Omega$ = 1000, and $R_0$ = 60, and the combined buoyancy parameter, $(Gr_\Omega/Re^2)R_0$, is of the order of unity.

**Flow and Heat Transfer Parameters**

The local skin friction coefficient $C_f = \mu(\partial u/\partial z)_w/(\rho u_{in}^2/2)$ and its mean value $\overline{C_f}$ can be written in dimensionless form, i.e.

$$C_f = \frac{2}{Re}\left(\frac{\partial U}{\partial Z}\right)_w \qquad \overline{C_f} = \frac{2}{R_0^2 - R_{in}^2}\int_{R_{in}}^{R_0} C_f R \, dR \tag{7}$$

The heat transfer performance is characterized by $Nu = hs/k$. Dimensionless expressions for the local and mean Nusselt numbers are

$$Nu = -\frac{1}{\theta_w - \theta_b}\left[\frac{\partial \theta}{\partial Z}\right]_w \qquad \overline{Nu} = \frac{2}{R_0^2 - R_{in}^2}\int_{R_{in}}^{R_0} NuR \, dR \tag{8}$$

Where $\theta_b = (T_b - T_r)/\Delta T_c$ is the dimensionless bulk temperature.

## Numerical Procedure

The parabolic system, Eqs. (1–5) with boundary conditions [Eq. (6)], was solved by using a typical marching technique. Owing to the large gradients in the entrance region, a nonuniform grid distribution in both the radial and axial directions was used to capture the radial development of the flow. The grid lines were more closely spaced near the inlet, and the grid size $\Delta R/(R_0 - R_{in})$ was varied from the order of $10^{-3}$ to $10^{-2}$. The outer boundary of the computational domain $R_0$ in this study was 60. A numerical experiment was performed to examine the grid dependence of the computational results. From the local Nusselt numbers listed in Table 1, it is obvious that a grid system of 101 × 41 is sufficient, which was used in the computations.

The system of equations was discretized to a linear system by the use of finite difference approximations. The method of solution involves a marching procedure in the radial direction and is implicit in the axial direction. The marching procedure proceeds continuously until the preset terminal location ($R_0$) is reached, or stops at the radial position where flow reversal occurs. The tri-diagonal matrix algorithm (TDMA) was employed for the solution of the resultant tridiagonal system. In the calculations the pressure can be determined by satisfying the global continuity. The iterative procedure in the axial direction is ended when the relative errors in the dependent variables $U$, $V$, $W$, and $\theta$ are all less than $10^{-4}$.

## Results and Discussion

In Fig. 2 the present predictions of local Nusselt numbers for the UWT case are compared with the elliptic solutions by Sim and Yang.[15] The solutions agree well for stationary parallel disks ($Ro$ = 0), but deviate slightly in the region near the entrance for the rotating case ($Ro$ = 0.0667). The discrepancy can be attributed to the different mathematical systems solved in the two studies. It is believed that the boundary-layer approximation in the present study, the low resolution of the elliptic solutions computed on a coarser grid system (30 × 15), and the possibility of premature fully developed conditions[15] are the influential factors.

**Table 1 Numerical experiments on grid dependence of local $Nu$ (UWT): $Re$ = 500, $Ro$ = 0.05, $Gr_\Omega$ = 500, $R_{in}$ = 20, $R_0$ = 60**

| $R'$ \ $M \times N$ | $Nu$ | | | | |
|---|---|---|---|---|---|
| | 201 × 81 | 101 × 81 | 101 × 41 | 101 × 21 | 51 × 21 |
| 1.100 | 6.773 | 6.760 | 6.757 | 6.737 | 6.663 |
| 4.103 | 4.337 | 4.381 | 4.380 | 4.373 | 4.362 |
| 8.021 | 3.727 | 3.740 | 3.739 | 3.735 | 3.755 |
| 15.032 | 3.623 | 3.636 | 3.635 | 3.631 | 3.654 |
| 25.449 | 3.903 | 3.913 | 3.911 | 3.905 | 3.918 |
| 37.323 | 4.338 | 4.342 | 4.342 | 4.333 | 4.337 |

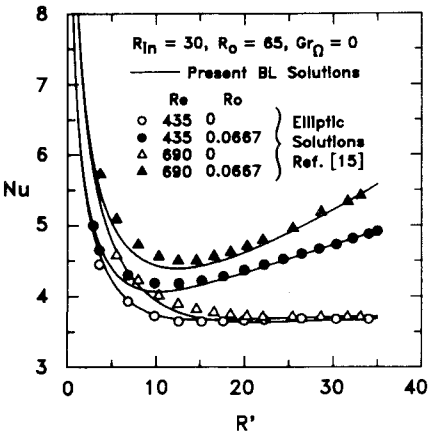


**Fig. 2 Comparison of the present predictions with Sim and Yang's results (UWT).**

**Isothermal Disk Solutions**

In Fig. 3a, a stationary case without rotational effects is presented as a reference. The velocity profiles are of the same type as those arising in forced convection problems except for the lower centerline velocity at the downstream location due to the enlargement of the flow area and the associated adverse pressure gradient. Coriolis effects on the development of the radial velocity are revealed in Figs. 3b, 3e, and 3c for $Ro$ = 0.02, 0.05, and 0.08. Note that with $Gr_\Omega$ = 0, the radial velocity near the centerline is accelerated near the entrance and retarded downstream by the Coriolis effect. This results in a shift of the peak of radial velocity profile from the center toward the wall, as can also be observed in Sim and Yang's results.[15] It is a consequence of the Coriolis effect due to the term $2RoV$. Near the wall the tangential velocity $v$ is larger than that near the centerline, and the Coriolis term $2\Omega v$ is therefore higher near the walls. This effect causes the fluid near the wall to accelerate and consequently shifts the radial velocity peak. If the rotational speed is further increased, a thinner highly viscous layer (Ekman layer) near the wall can be expected, and the radial velocity profile thus becomes more concave near the centerline. In this situation high skin friction and heat transfer rate result.

From the results shown in Figs. 3d, 3e, and 3f it can be seen that the centrifugal-buoyancy effect alters the velocity fields through the variation of the governing parameter $Gr_\Omega$. In buoyancy-opposed flow $Gr_\Omega > 0$ in Fig. 3d, the fluid near the disk is retarded by the centrifugal-buoyancy effect. By comparing the profiles in Figs. 3d and 3e at the same downstream location (e.g., $R'$ = 34.801 where the remarkable centrifugal-buoyancy effect is presented) it can be seen that the central parts of the radial velocity profiles for $Gr_\Omega > 0$ have to be increased to maintain the global continuity. On the contrary, in buoyancy-assisted flow $Gr_\Omega < 0$ in Fig. 3f, the fluid near the wall is accelerated and the central parts of the velocity profiles are flattened due to buoyancy. Also, from Fig. 3f it is obvious that the interaction of Coriolis and buoyancy-assisting effects may enhance the flow near the wall. For buoyancy-opposed flow (Fig. 3d) the Coriolis effect is diminished by the centrifugal buoyancy.

Figure 3 also shows that the centerline velocity increases due to the high diffusion in the entrance region and subsequently decreases due to the enlargement of the flow passage

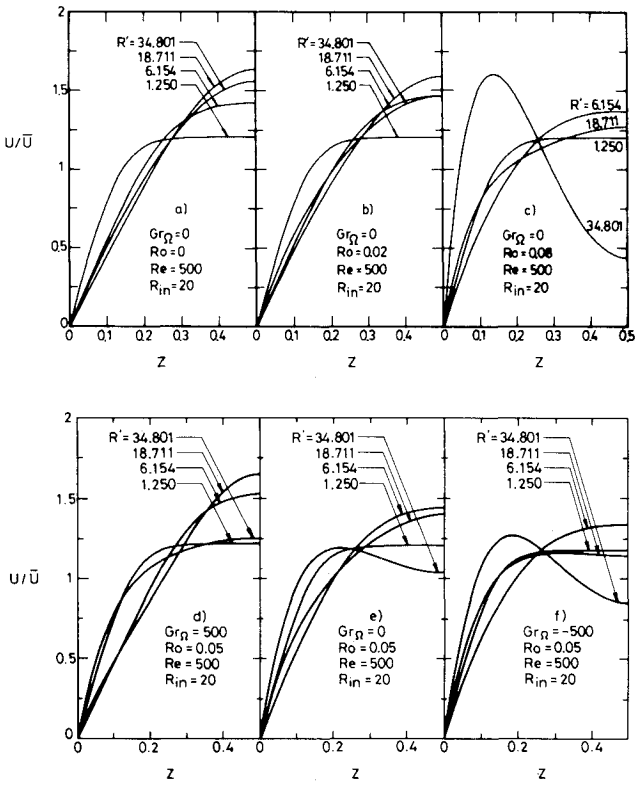


Fig. 3 Radial velocity profiles under various conditions (UWT).

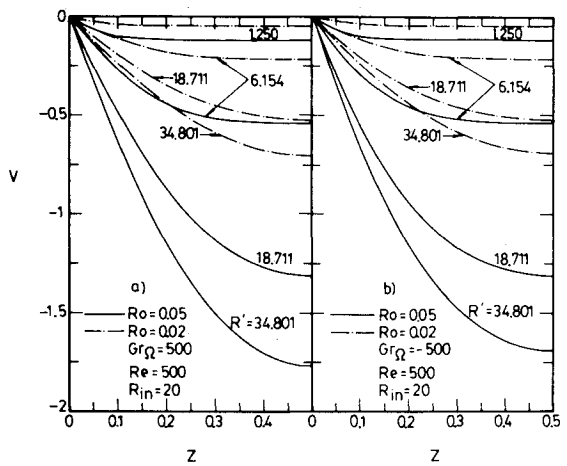


Fig. 4 Tangential velocity distributions (UWT).

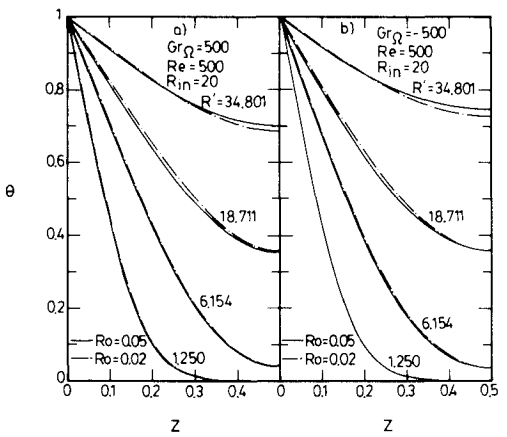


Fig. 5 Temperature distributions in various rotational conditions (UWT).

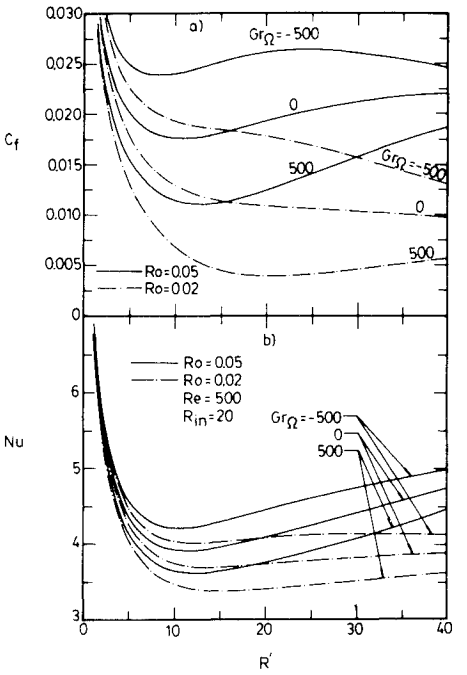


Fig. 6 Centrifugal-buoyancy effect on local $C_f$ and $Nu$ (UWT).

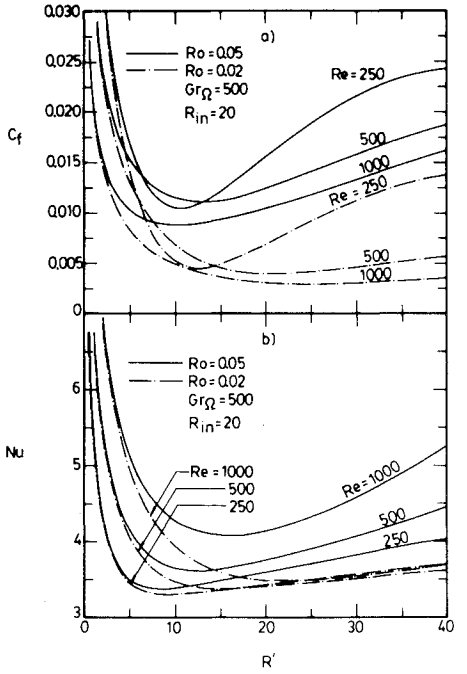


Fig. 7 Through-flow effect on local $C_f$ and $Nu$ (UWT).

and the Coriolis effect as mentioned above. Since the higher Coriolis force can build a radial velocity peak near the disk, the radial velocity profile has to become concave near the center to satisfy the global continuity. Moreover, it is observed that (e.g., Figs. 3b and 3e) the centerline velocities for $Ro$ = 0.02 and $Ro$ = 0.05 deviate from each other downstream. Also, as the strength of the Coriolis effect in the radial direction depends on the nonuniformity of the tangential velocity distribution; the growth of the Coriolis effect along the radial direction can be attributed to the increasing nonuniformity of the tangential velocity $v$ as shown in Fig. 4. It is seen from Fig. 4 that the tangential velocity profile depends strongly on the rotation number but is only slightly influenced by the buoyancy. However, both the effects of Coriolis and centrifugal buoyancy on the temperature function $\theta$ are not very critical as shown in Fig. 5.

Figures 6 and 7 show the effects of buoyancy and through-flow on the local skin friction and heat transfer rate in the developing flow region. It is obvious that the buoyancy-assisting effect ($Gr_\Omega < 0$) enhances the heat transfer rate, but with the penalty of high skin friction. Conversely, the buoyancy-opposing effect decreases both. The skin friction is large for a small Reynolds number $Re = 250$ as shown in Fig. 7, and becomes smaller as $Re$ increases. On the other hand, a strong forced flow provides a large forced convection effect. Therefore, $Nu$ increases with an increase in the through-flow Reynolds number.

**Comparisons Between Isothermal Disk and Isoflux Disk Solutions**

In this section results for a uniform heat flux boundary condition are presented and comparisons between the results from the isothermal disk (UWT) and isoflux disk (UHF) solutions are made. Figure 8 shows the $U/\bar{U}$ profiles from the UHF solution under the influence of centrifugal buoyancy. The velocity distributions in Figs. 8a and 8b are the counterpart of those in Figs. 3d and 3f. In comparing the two sets of solutions it is found that the velocity profiles are only slightly different, i.e., the developments of the radial velocities for both UWT and UHF conditions are quite similar.

However, one might expect that the temperature fields are very different between the two heating conditions. As shown in Fig. 9, the wall-to-fluid temperature difference (WFTD), a measure of temperature field nonuniformity, is finite and seems to approach a constant at large $R'$. For isothermal disks the wall temperature remains constant but the fluid temperature rises continuously along the radial direction as shown in Fig. 5. As a result, the WFTD is reduced and approaches zero as the fluid flows radially outward. Since the local effect of centrifugal buoyancy is closely related to the temperature distribution in the $Z$-direction, it can be inferred that the influences of buoyancy in UHF and UWT cases are different.

A comparison of the local skin-friction and the local heat transfer rate between UWT in Fig. 6 and UHF in Fig. 10 shows that at the downstream location (large $R'$), the centrifugal-buoyancy effect on the local values of $C_f$ and $Nu$ is suppressed in the UWT case due to the diminishing WFTD. The buoyancy effect is relatively stronger in the UHF case, however, because of the higher WFTD. It is noted that from Eq. (2), the local buoyancy force depends on the parameter $-(Gr_\Omega/Re^2)$, the radial position $R$, and the temperature function $\theta(R, Z)$. With fixed rotation and flow conditions, the temperature field becomes a dominant factor for the strength of the centrifugal-buoyancy effect. As an example, consider the two buoyancy-assisted heat transfer curves with $Gr_\Omega = -500$ and $Ro = 0.02$ in Figs. 6 and 10, respectively. The local heat transfer rate for both UWT and UHF conditions increases downstream of the radial location $R' = 10$. The growing trend comes from the increasing radial distance $R$ or centrifugal force $R\Omega^2$. However, the heat transfer rate for isoflux disk is higher than that for isothermal disk due to the relatively larger WFDT or temperature nonuniformity. Nevertheless, in the buoyancy-opposed flow with $Gr_\Omega > 0$, the growing trend is flattened by the large effect of centrifugal buoyancy (see Fig. 10b).

Figures 11a and 11b show the mean skin friction and the mean heat transfer rate for the UWT and UHF cases, re-

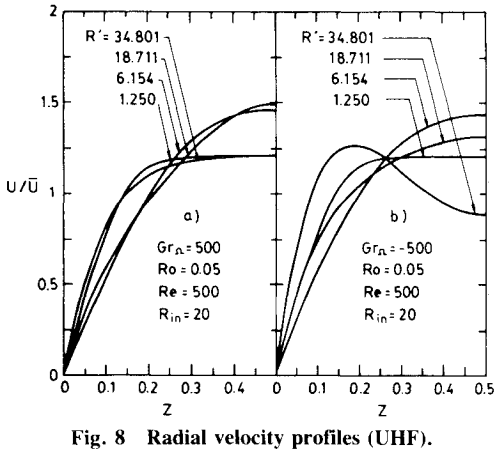


Fig. 8 Radial velocity profiles (UHF).

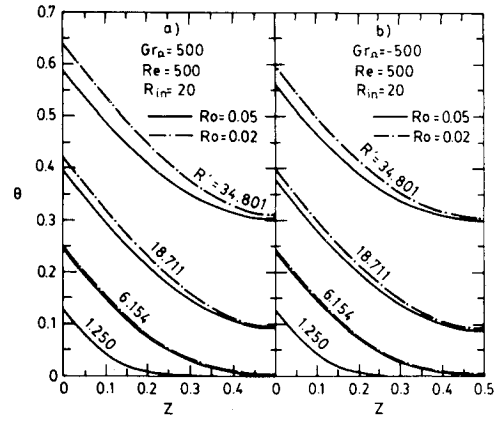


Fig. 9 Temperature distributions (UHF).

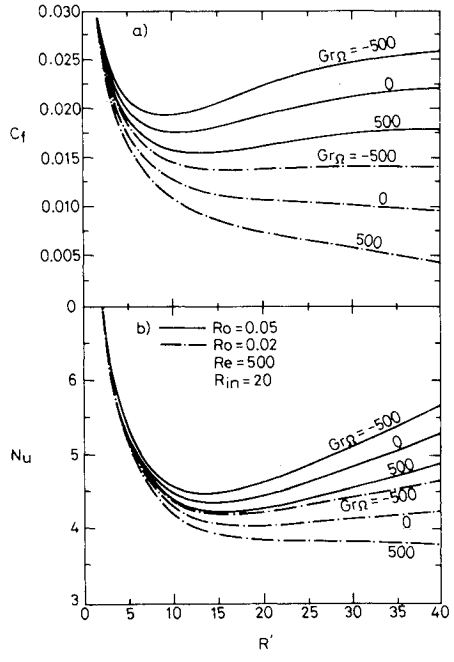


Fig. 10 Centrifugal-buoyancy effect on local $C_f$ and $Nu$ (UHF).

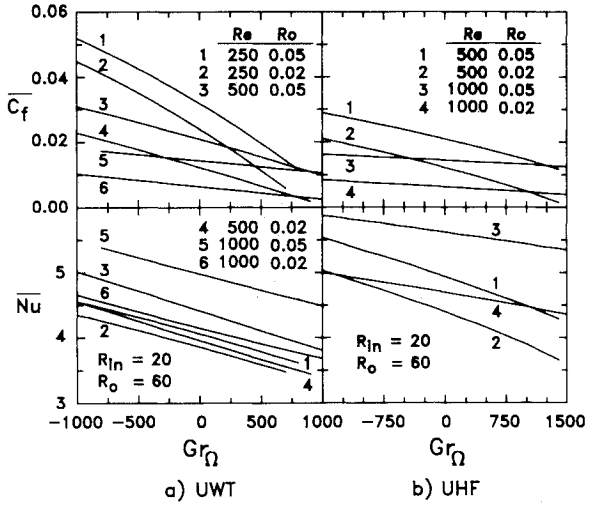


Fig. 11 Mean skin friction and heat transfer parameters: a) isothermal disks (UWT), and b) isoflux disks (UHF).

spectively. Comparing the curves 3, 4, 5, and 6 for the UWT in Fig. 11a and the counterpart curves 1, 2, 3, and 4 for the UHF in Fig. 11b, the mean skin-friction under the two wall-heating conditions are slightly different; but the differences in the heat transfer performance are more noticeable. Under the same flow and rotational conditions, it can be seen that the mean heat transfer rate is higher for the UHF case than for the UWT case due to the larger WFTD in the former case. Under either UWT or UHF condition, the effect of centrifugal buoyancy on $\overline{C_f}$ is larger than that on $\overline{Nu}$ due to the larger sensitivity of the velocity field to the buoyancy effect. Also, at lower Reynolds numbers ($Re$ = 250 and 500), the influences of the centrifugal buoyancy are larger than that at the higher value ($Re$ = 1000), because the buoyancy force is relatively higher than that in the latter due to the smaller forced convection effect.

## Concluding Remarks

Simultaneously developing flow and heat transfer in laminar mixed-convection regime between two symmetrically heated corotating disks has been studied numerically. From the predictions presented some conclusions can be drawn.

The rotation-induced buoyancy effect does alter the flow and heat transfer characteristics and should be considered in this class of convection problems. For radially outward flow the heat transfer rate is decreased by the buoyancy-opposing effect at $Gr_\Omega > 0$. Conversely, the heat transfer rate can be enhanced in the presence of the buoyancy-assisting effect at $Gr_\Omega < 0$. For the present geometry and flow conditions buoyancy can induce apparent influences in the flow and heat transfer characteristics. For example, at $Re$ = 500, $Ro$ = 0.05, $|Gr_\Omega|$ = 1000, and $R_0$ = 60, the buoyancy effect may result in a change of about 50% in the mean skin friction and more than 10% in the mean Nusselt numbers. At high rotation numbers the velocity peak tends to move toward the disk wall and form a high-gradient layer. Accordingly, the Coriolis term ($2\Omega V$) always increases the skin friction and the heat transfer rate. Increasing through-flow Reynolds number increases the heat transfer rate and lowers the skin friction coefficient, but it suppresses the rotational effects.

No previous experimental work has considered the centrifugal-buoyancy effect in corotating disk problems, and even in pure forced convection studies the measured data by various groups are still inconsistent (as mentioned in Ref. 19). Therefore, there are no data available (at various $Gr_\Omega$) with which the present numerical predictions can be compared. However, the present results can serve as a theoretical basis for qualitatively evaluating the significance of the centrifugal-buoyancy effect in a rotating disk system. A well-designed and carefully conducted experiment for the system considered here would be very appropriate.

## References

[1]Kapinos, V. M., Pustovalov, V. N., and Rud'ko, A. P., "Heat Transfer During the Flow of a Medium from the Center to the Periphery Between Two Rotating Disks," *Heat Transfer—Soviet Research*, Vol. 5, No. 1, 1973, pp. 1–9.

[2]Owen, J. M., and Bilimoria, E. D., "Heat Transfer in Rotating Cylindrical Cavities," *Journal of Mechanical Engineering Science*, Vol. 19, No. 4, 1977, pp. 175–187.

[3]Owen, J. M., "Fluid Flow and Heat Transfer in Rotating Disc Systems," International Centre for Heat Transfer Series, *Heat and Mass Transfer in Rotating Machinery*, edited by D. E. Metzger and N. H. Afgan, Hemisphere, Washington, DC, 1984, pp. 81–103.

[4]Chew, J. W., "Computation of Forced Laminar Convection in Rotating Cavities," *Journal of Heat Transfer*, Vol. 107, May 1985, pp. 277–282.

[5]Mochizuki, S., and Yang, W. J., "Heat Transfer and Friction Loss in Laminar Radial Flows Through Rotating Annular Disks," *Journal of Heat Transfer*, Vol. 103, May 1981, pp. 212–217.

[6]Yang, W. J., "Gas-Liquid Mass Transfer in Rotating Performance Disc Contactors," *Letters in Heat and Mass Transfer*, Vol. 9, pp. 119–129.

[7]Chang, C. J., Schuler, C. A., Humphrey, J. A. C., and Greif, R., "Flow and Heat Transfer in the Space Between Two Corotating Disks in an Axisymmetric Enclosure," *Journal of Heat Transfer*, Vol. 111, Aug. 1989, pp. 625–632.

[8]Owen, J. M., and Rogers, R. H., *Flow and Heat Transfer in Rotating-Disc Systems, Vol. 1: Rotor-Stator Systems*, Wiley, New York, 1989, Chaps. 5 and 8.

[9]Siegel, R. "Analysis of Buoyancy Effect on Fully Developed Laminar Heat Transfer in a Rotating Tube," *Journal of Heat Transfer*, Vol. 107, May 1985, pp. 338–344.

[10]Soong, C. Y., and Hwang, G. J., "Laminar Mixed Convection in a Radially Rotating Semiporous Channel," *International Journal of Heat and Mass Transfer*, Vol. 33, No. 9, 1990, pp. 1805–1816.

[11]Soong, C. Y., *Convective Heat Transfer in Radially Rotating Channels*, Ph.D. Dissertation, Dept. of Power Mech. Engrg., National Tsing Hua Univ., Hsinchu, Taiwan, Republic of China, 1991.

[12]Morris, W. D., and Ayhan, T., "Observation on the Influence of Rotation on Heat Transfer in the Coolant Channel of Gas Turbine Rotor Blades," *Proceedings of Institution of Mechanical Engineering*, Vol. 193, No. 21, 1979, pp. 303–311.

[13]Soong, C. Y., Lin, S. T., and Hwang, G. J., "An Experimental Study of Convective Heat Transfer in Radially Rotating Rectangular Ducts," *Journal of Heat Transfer*, Vol. 113, No. 3, 1991, pp. 604–611.

[14]Raal, J. D., "Radial Source Flow Between Parallel Disks," *Journal of Fluid Mechanics*, Vol. 85, Pt. 3, 1978, pp. 401–416.

[15]Sim, Y. S., and Yang, W. J., "Numerical Study on Heat Transfer in Laminar Flow Through Co-Rotating Parallel Disks," *International Journal of Heat Mass Transfer*, Vol. 27, No. 11, 1984, pp. 1963–1970.

[16]Morris, M. D., *Heat Transfer and Fluid Flow in Rotating Coolant Channels*, Wiley, Chichester, 1981, Chap. 2.

[17]Mochizuki, S., and Yang, W. J., "Local Heat Transfer Performance and Mechanisms in Radial Flow Between Parallel Disks," *Journal of Thermophysics and Heat Transfer*, Vol. 1, No. 2, 1987, pp. 112–116.

[18]Mochizuki, S., and Inoue, T., "Self-Sustained Flow Oscillations and Heat Transfer in Radial Flow Through Co-Rotating Parallel Disks," *Experimental Thermal Fluid Science*, Vol. 3, No. 2, 1990, pp. 242–248.

[19]Suryanarayana, N. V., Scofield, T., and Kleiss, R. E., "Heat Transfer to a Fluid in Radial, Outward Flow Between Two Coaxial Stationary or Corotating Disks," *Journal of Heat Transfer*, Vol. 105, No. 3, 1983, pp. 519–526.